Original papers
Advanced structural materials, materials for extreme conditions

УДК 621.791.13 DOI: 10.17277/jamt-2025-10-02-108-116

Study of the influence of titanium interlayer on formation of AlMg6 – 12Cr18Ni10Ti weld interface during explosive welding

© Andrey Yu. Malakhov[a], Stepan A. Seropyan[a]✉, Igor V. Denisov[a], Denis V. Shakhray[b], Olga D. Boyarchenko[a], Nemat N. Niyozbekov[a], Evgenii I. Volchenko[a]

[a] *Merzhanov Institute of Structural Macrokinetics and Materials Science, Russian Academy of Science, 8, Academician Osipyan St., Chernogolovka, 142432, Russian Federation,*
[b] *Federal Research Center of Problems of Chemical Physics and Medicinal Chemistry of Russian Academy of Sciences, 1, Academician Semenova Av., Chernogolovka, 142432, Russian Federation*

✉ stepan.seropyan@yandex.ru

Abstract: This paper presents the aspects of the formation of multilayer composite material (MCM) consisting of aluminium-magnesium alloy AlMg6, titanium VT1-0 and austenitic stainless steel 12Cr18Ni10Ti during explosive welding. This MCM has promising properties for use in various industries such as shipbuilding and automobile manufacturing. However, the production of this material presents certain difficulties due to different properties of the initial materials. In this paper, the effect of residual stresses occurring in MCM after explosive welding on the continuity of the joint was investigated. Using metallographic studies and electron microscopy, it was found that the high velocity impact process between different materials comprising MCM formed weld interfaces with straight and wavy profiles. There was also evidence of dynamic recrystallisation at the 12Cr18Ni10Ti–VT1-0 weld interface and the formation of vortex zones in wave crests. The microhardness of the layers was also measured. The measurement showed that hardening occurred in MCM layers with the maximum value in the 12Cr18Ni10Ti steel layer. The evaluation of tear strength revealed that the formation of cracks occurred at the interface between the VT1-0–AlMg6 weld interface, with an average strength of 160 MPa. The results of the study may be useful to specialists in materials science, mechanical engineering and other related fields.

Keywords: explosive welding; AlMg6; titanium; microhardness; weld interface; steel.

For citation: Malakhov AYu, Seropyan SA, Denisov IV, Shakhray DV, Boyarchenko OD, Niyozbekov NN, Volchenko EI. Study of the influence of titanium interlayer on formation of AlMg6 – 12Cr18Ni10Ti weld interface during explosive welding. *Journal of Advanced Materials and Technologies*. 2025;10(2):108-116. DOI: 10.17277/jamt-2025-10-02-108-116

Исследование влияния титана на образование соединения АМг6 – 12Х18Н10Т в процессе сварки взрывом

© А. Ю. Малахов[a], С. А. Серопян[a]✉, И. В. Денисов[a], Д. В. Шахрай[b], О. Д. Боярченко[a], Н.Н. Ниезбеков[a], Е.И. Волченко[a]

[a] *Институт структурной макрокинетики и проблем материаловедения им. А. Г. Мержанова РАН, ул. Академика Осипьяна, 8, Черноголовка, 142432, Российская Федерация,*
[b] *Федеральный исследовательский центр проблем химической физики и медицинской химии РАН, пр. Академика Семенова, 1, Черноголовка, 142432, Российская Федерация*

✉ stepan.seropyan@yandex.ru

Аннотация: Рассматриваются особенности формирования в процессе сварки взрывом многослойного композиционного материала (МКМ), состоящего из алюминиево-магниевого сплава АМг6, титана ВТ1-0 и аустенитной коррозионностойкой стали 12Х18Н10Т. Данный МКМ обладает перспективными свойствами для использования в различных отраслях промышленности, таких как судостроение и автомобильная

промышленность. Однако процесс получения такого материала сопряжен с определенными трудностями, связанными с различиями в свойствах исходных материалов. Проведено исследование влияния остаточных напряжений, возникающих в МКМ после сварки взрывом, на сплошность соединения. С помощью металлографических исследований и электронной микроскопии обнаружено, что в процессе высокоскоростного соударения между различными материалами, входящими в состав МКМ, формируются границы соединения с прямым и волнообразным профилем. Кроме того, получены данные о динамической рекристаллизации на границе соединения 12Х18Н10Т – ВТ1-0 и образовании вихревых зон в гребнях волн. Проведено измерение микротвердости слоев, которое показало, что в слоях МКМ произошло упрочнение, максимальное значение которого зафиксировано в слое из стали 12Х18Н10Т. Испытание прочности слоев на отрыв выявило, что разрушение происходило по границе соединения ВТ1-0 – АМг6 при средней прочности 160 МПа. Результаты исследования могут быть полезны для специалистов в области материаловедения, машиностроения и других смежных областей.

Ключевые слова: сварка взрывом; АМг6; титан; микротвердость; граница соединения; сталь.

Для цитирования: Malakhov AYu, Seropyan SA, Denisov IV, Shakhray DV, Boyarchenko OD, Niyozbekov NN, Volchenko EI. Study of the influence of titanium interlayer on formation of AlMg6 – 12Cr18Ni10Ti weld interface during explosive welding. *Journal of Advanced Materials and Technologies*. 2025;10(2):108-116. DOI: 10.17277/jamt-2025-10-02-108-116

1. Introduction

Multilayer composite materials (MCM) consisting of aluminum alloy and steel are widely used in shipbuilding, automobile and railcar manufacturing due to their high specific strength and corrosion resistance [1, 2].

Currently, the most common technologies for producing steel/aluminum alloy pairs are mechanical connections (e.g. riveting, clamping, etc.) and adhesive connections [3]. Mechanical and adhesive connections are inferior in strength per unit area to direct metal connections between sheets of steel and aluminum alloy [4].

One of the technologies that allows obtaining a metallic connection between aluminum alloys and steels is explosive welding (EW) [5–7]. This technology uses the energy of explosives to accelerate a metal sheet called a projectile and collide it with a stationary sheet called a base sheet at high speed. During the collision, the surfaces of the sheets are cleaned of any oxides and contaminants, thereby providing a metallic connection.

However, due to the significant difference in the properties of aluminum alloys, and in particular aluminum-magnesium and steel, it is problematic to obtain a strong connection. First of all, this is due to the formation of brittle intermetallic phases of the Fe_xAl_y type at the boundary of the welded joint [8, 9]. For example, in [10], a bimetallic material of aluminum alloy Al1100 with low-carbon steel was obtained. Two types of intermetallic phases Al_3Fe and Al_5Fe_2 were formed at the boundary of the joint. To reduce the formation of intermetallic phases at the interface of the aluminum alloy and steel, an interlayer is used [4]. Typically, ductile materials, pure aluminum, titanium, etc., act as an interlayer, which allow achieving high strength and ductility of the material [4, 11]. The use of an interlayer of refractory materials (tantalum, vanadium, titanium, etc.) helps prevent the formation of intermetallic compounds during heating during further technological processing and operation of the product [2]. For example, in [11], the authors showed that a titanium interlayer prevents the formation of brittle intermetallic phases Fe_xAl_y. Moreover, intermetallic phases Ti_xAl_y are formed, which have a higher initial temperature and a longer growth time than Fe_xAl_y.

A review of the work shows that most studies of EW were carried out for aluminum alloys with a magnesium content of less than 5 %. Explosion welding of AlMg6 with stainless steel and titanium has not been sufficiently studied.

The aim of the work was to study the influence of the titanium interlayer on the microstructure and mechanical properties of AlMg6–12Cr18Ni10Ti.

2. Materials and Methods

2.1. Initial materials

The following source materials were used to obtain MCM: base sheet – aluminum-magnesium alloy AlMg6 (4×200×300 mm); interlayer – titanium VT1-0 (1×200×300 mm), rolled sheet – austenitic corrosion-resistant steel 12Cr18Ni10Ti (3×200×300 mm).

Table 1 shows physical and mechanical properties of the source materials, such as density (ρ), melting point (T_m), yield strength σ_y, tensile strength σ_t, Brinell hardness (HB) and relative elongation (δ).

Table 1. Physical and mechanical properties of the source materials

Material	Thickness, mm	ρ, kg·m^{-3}	T_m, °C	σ_y, MPa	σ_t, MPa	HB	δ, %
AlMg6	4	2640	630	160	350–355	81	17.9–20.7
Titanium	1	4500	1670	–	395–400	163	67–71
12Cr18Ni10Ti	3	7900	1450	205	530	106	52–56

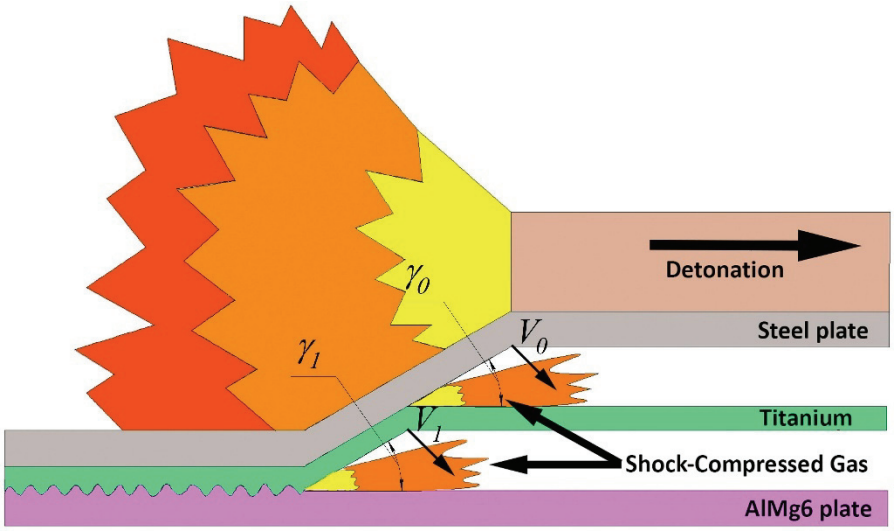

Fig. 1. Experimental scheme of the explosive welding experiment

The microstructure of AlMg6 consists of the α-phase with a grain size of ~50 μm and the β-phase of Mg_2Al_3 located mainly along the grain boundaries of the α-phase. AlMg6 contains insoluble inclusions of the type (Fe, Mn). The microstructure of 12Cr18Ni10Ti consists of austenite with a small amount of ferrite. The size of the austenite grains is 30–40 μm throughout the thickness of the material. The microstructure of titanium mainly consists of the α-phase, which has a fine-grained structure with a grain size of 7 to 20 μm [12].

2.2. Production of multilayer composite materials

The experimental scheme for obtaining MCM is shown in Fig. 1. A mixture of ammonium nitrate and diesel fuel was used as explosive.

The parameters of EW were calculated using formulas (1) and (2) [13]:

$$V_0 = 1.2D\frac{\sqrt{1+\frac{32}{27}r-1}}{\sqrt{1+\frac{32}{27}r+1}}; \quad (1)$$

Table 2. Explosive welding parameters of AlMg6 + + Titanium + 12Cr18Ni10Ti

D, m·s^{-1}	V_0/V_1, m·s^{-1}	r	γ_0/γ_1, °
2600	686/508	1,16	13,8/10,7

$$\gamma = 2\arcsin\left(\frac{V_0}{2D}\right), \quad (2)$$

where V_0 is the velocity of the plate being thrown; D is the detonation velocity of the explosive; r is a dimensionless parameter equal to the ratio of the mass of the explosive charge to the mass of the plate being thrown, γ is the impact angle.

The design parameters of EW are presented in Table 2.

2.3. Quality control methods for welded joints

Ultrasonic testing (UT) was performed using a UD2 BP flaw detector with a DF5012 sensor to assess the continuity of the welded joint. Ultrasonic testing was performed in 3 stages: after EW, 14 days after EW and after heat treatment (HT). HT was

performed in an SNOL 8.2/1100 electric muffle furnace at a temperature of 450 °C and held for 1 hour while cooling with the furnace.

Samples for metallographic testing were cut using a DK7725 electrical discharge machine from areas with satisfactory weld continuity in accordance with the ultrasonic testing maps. The samples were ground on abrasive paper with a grain size of 120 to 2500, then polished on felt with diamond paste with a grain size of 1–2 μm on a LAP-1000 automatic grinding and polishing machine. Final polishing was performed on an AEP 2.2 electrochemical polishing machine.

Metallographic testing of sections was performed on a METAL LV-34 optical microscope. The images were obtained using an MC-5.3 camera. Microhardness was measured using the Vickers method on a PMT-3M microhardness tester under a load of 50 g using the MMC-Hardness software package. Energy dispersive microanalysis of structural components was performed on a Zeiss ULTRA plus electron microscope with an INCA 350 XT Oxford Instruments attachment for X-ray microanalysis. The tear strength of the samples was studied on an Instron 1195 universal testing machine. Samples for metallographic studies and tear strength studies were selected according to the corresponding schemes presented in [12].

3. Results and Discussion

After the UT, maps were compiled (Fig. 2), where the continuity zones are shown as green areas. The continuity of the joint after the UT was 35 % of the total plate area (Fig. 2*a*).

After the EW, residual stresses arise in the material. They arise as a result of local deformations of the metal due to uneven heating during EW. Residual stresses are mainly concentrated at the weld interface [14]. If the level of residual stresses exceeds the strength of the joint, this can lead to delamination of the material. To determine the effect of residual stresses on the continuity of the joint, UT was carried out immediately after the UT and 14 days after the UT experiments. In the second case, the continuity of the joint was about 30 % of the total plate area (Fig. 2*b*). The presence of residual stresses in the material led to a decrease in the continuity of the joint.

Subsequent maintenance and UT showed that the continuity of the joint did not change. Thus, it can be concluded that within 14 days, complete relaxation of residual stresses occurs in the weld joint boundary area.

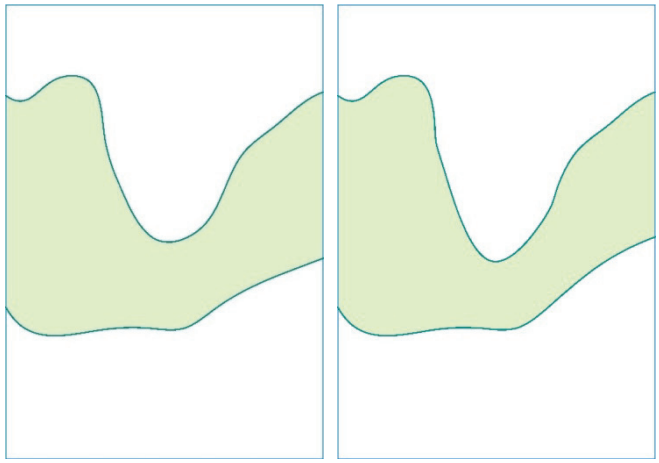

(a) *(b)*

Fig. 2. Ultrasonic testing maps of joint continuity: *a* – immediately after EW; *b* – 14 days after EW

Further studies of the microstructure were carried out on samples after the HT. It is known that during the HT process, new phases can form at the boundary of the connection of dissimilar materials, which can affect the properties of the connection [15–17].

Figure 3 shows the boundary of the 12Cr18Ni10Ti – Titanium – AlMg6 joint, which has a rectilinear profile between AlMg6 and titanium, and a wave-like profile between titanium and 12Cr18Ni10Ti. The wavelength at the boundary of the 12Cr18Ni10Ti – titanium joint is about 150 μm, and the height is about 25 μm.

Figure 4 shows the microstructure of the 12Cr18Ni10Ti-Titanium joint boundary [18, 19]. During the EW process, vortex zones were formed (area 1), around which dynamic recrystallization

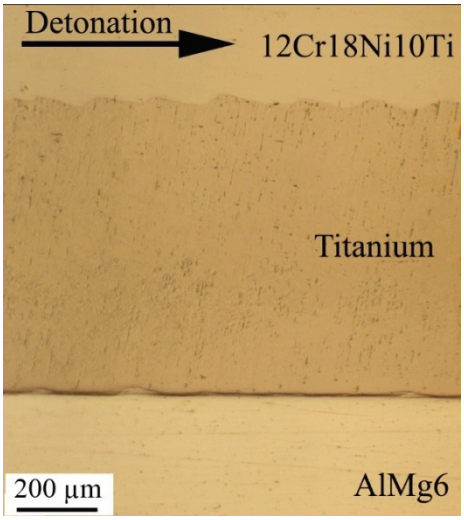

Fig. 3. Weld interface of 12Cr18Ni10Ti – Titanium – AlMg6

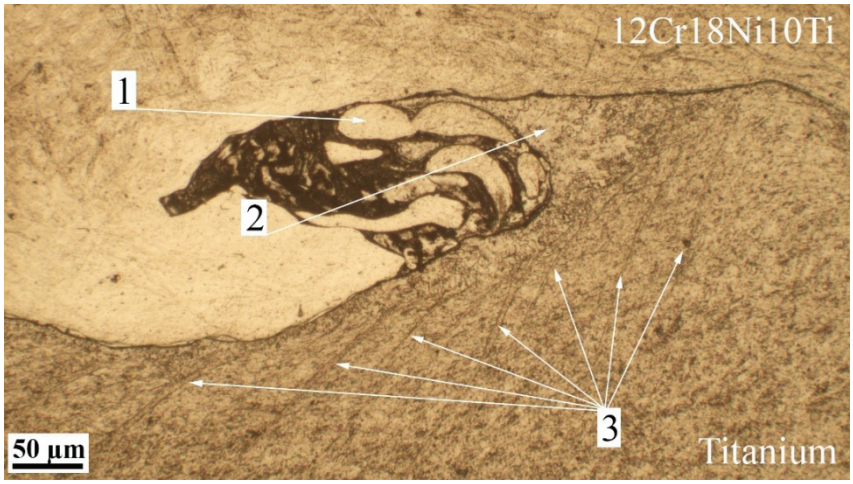

Fig. 4. Microstructure of 12Cr18Ni10Ti – Titanium weld interface

zones were found (area 2). It is known that a large amount of heat is released in the vortex zones, which promotes the formation of dynamic recrystallization zones in titanium. This process is typical for materials with low thermal conductivity [18, 19].

Localized shear bands (LSB) were also found (area 3). LSBs were formed in titanium at the joint boundary, at an angle of approximately 45°. It is known that LSBs are one of the failure mechanisms that occur in some materials at high deformation rates, for example, during EW. This term describes a sharp increase in temperature and the transfer of heat to a narrow region [20].

Figure 5 shows the microstructure and EDS analysis results of the weld interface. The results show that the titanium interlayer limits mutual diffusion between 12Cr18Ni10Ti and AlMg6 (Fig. 5*a*). The vortex zone consists of areas of brittle

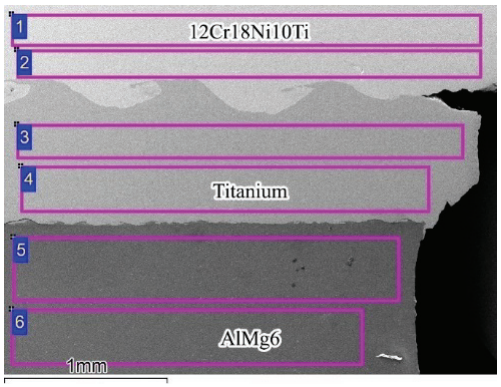

No.	Element content, at. %							
	O	Mg	Al	Si	Ti	Cr	Fe	Ni
1	2	0.4	3.3	0.8	0.5	18.4	65.3	9.3
2	3	0.1	2.3	1.5	0.4	18.3	64.6	9.8
3	–	–	2.3	–	97.5	0.1	0.1	–
4	–	0.2	2	–	97.3	–	0.2	0.3
5	4.1	6.7	88.7	0.3	–	–	0.2	–
6	2	6.7	91.2	–	–	–	0.1	–

(a)

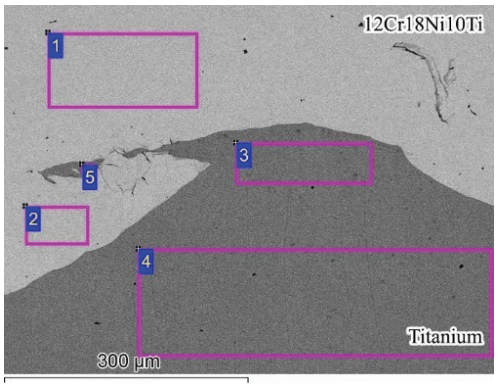

No.	Element content, at. %				
	Al	Ti	Cr	Fe	Ni
1	3.2	0.3	18.8	67.4	10.3
2	3.4	0.3	18.9	67.7	9.7
3	1.9	97.7	0.1	0.2	0.1
4	2.6	97.2	0.2	–	–
5	2.4	96.8	0.1	0.5	0.2

(b)

Fig. 5. SEM-images and results of EDS analysis of MCM 12Cr18Ni10Ti – Titanium – AlMg6:
a – microstructure MCM; *b* – vortex zone of weld interface 12Cr18Ni10Ti – Titanium

intermetallic phases and a mechanical mixture of titanium with elements of corrosion-resistant steel 12Cr18Ni10Ti (Fig. 5*b*, No. 5). Such a structure is usually observed in pairs of materials with close density values, such as Al/Al [21], steel/steel [22].

Figure 6 shows the microstructure of the interface between 12Cr18Ni10Ti and titanium. During EW, a melted zones of about 3 μm thickness was formed at the interface. According to the Fe–Ti phase diagram and the results of EDS analysis (Fig. 6, point 2), it was established that the molten layer consists of the brittle intermetallic phase TiFe [23].

Figure 7 shows the Titanium – AlMg6 bond boundary. During the EW process, a melted zone up to 20 μm thick was formed (Fig. 7*a*). The results of the EDS analysis showed that the melt consists of titanium particles surrounded by the AlMg6 alloy (Fig. 7*b*).

The study of the MCM microhardness showed that near the boundary of the 12Cr18Ni10Ti – Ttitanium joint an increase in microhardness occurs, which is associated with the formation of a hardening zone with a width of about 200 μm (Fig. 8).

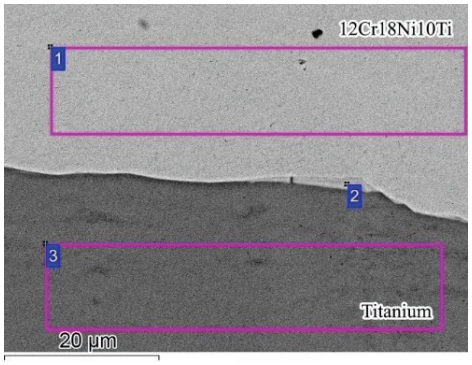

No.	Element content, at. %					
	Al	Si	Ti	Cr	Fe	Ni
1	2.6	1.4	0.9	18	67.5	9.6
2	2.9	0.9	40.6	11.4	37.9	6.3
3	2.2	0.4	97.1	0.1	0.1	0.1

Fig. 6. SEM-images and results of EDS analysis of weld interface 12Cr18Ni10Ti – Titanium

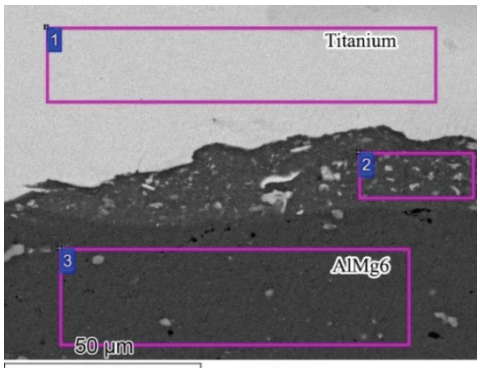

No.	Element content, at. %			
	O	Mg	Al	Ti
1	13.6	0.2	2	84.2
2	14	6	75.3	4.7
3	3.2	6.4	90.4	–

(a)

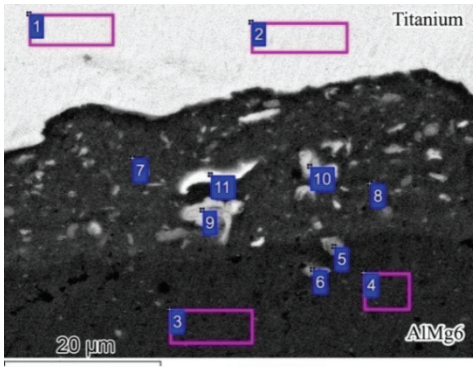

No.	Element content, at. %				
	O	Mg	Al	Ti	Fe
1	8.1	–	1.9	89.8	0.2
2	13.9	0.2	2	83.9	–
3	2.2	6.1	91.6	0.1	–
4	2.6	5.8	91.5	0.1	–
5	1.1	4	90	1.4	3.5
6	3.1	5.2	88	0.2	3.5
7	3.8	6.6	85.9	3.5	0.2
8	10	6.4	80.7	2.9	–
9	3.7	3.5	50.2	42.6	–
10	14.5	3.9	47.9	33.7	–
11	8	2.6	21.8	67.5	0.1

(b)

Fig. 7. SEM-images and results of EDS analysis of weld interface Titanium – AlMg6:
a – microstructure weld interface; *b* – microstructure of melted zone

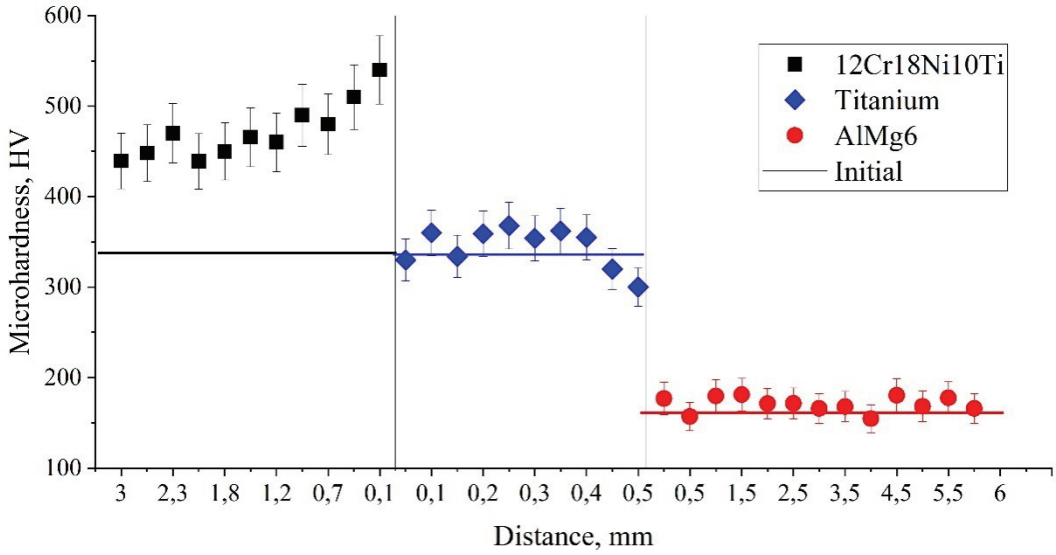

Fig. 8. Microhardness of 12Cr18Ni10Ti – Titanium – AlMg6

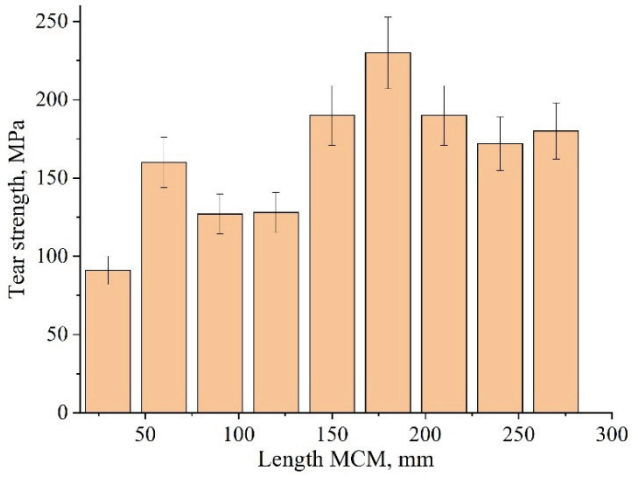

Fig. 9. Tear strength distribution along the MCM length

Figure 9 shows a graph of the strength distribution along the MCM length. It is evident from the graph that the strength value is unevenly distributed along the MCM length. As the distance from the initiation point increases, the strength of the joint increases to 230 MPa, and from a distance of 200 mm it decreases to 172 MPa, which is apparently due to the spread of explosives and the influence of unloading waves. At the same time, the average tear strength was 160 MPa. The destruction of the samples occurred along the titanium-AlMg6 joint boundary.

4. Conclusion

In the course of the work, a multilayer composite material consisting of 12Cr18Ni10Ti, titanium and AlMg6 layers was obtained using the EW method. As a result of the study, it was found that the continuity zone of the welded joint is located in the central part of the multilayer composite material and occupies 35 % of the total area of the material. It is shown that after EW, the continuity of the joint is affected by residual stresses, which over time lead to a decrease in the area of the continuity of the joint. The study of the microstructure of the multilayer composite material showed that the boundary of the joint between AlMg6 and titanium has a rectilinear profile, and between titanium and 12Cr18Ni10Ti – wavy with a length of 150 μm and a height of 25 μm. At the boundary of the 12Cr18Ni10Ti – titanium joint, areas of dynamic recrystallization and vortex zones with plastically deformed layers around them are observed at the tops of the waves. It was found that melted areas were formed at the AlMg6-titanium joint boundary, which were titanium particles surrounded by AlMg6 alloy.

It was revealed that in the 12Cr18Ni10Ti steel layer near the joint boundary, hardening occurred to a depth of ~200 μm. The average tear strength of the multilayer composite material was 160 MPa.

Thus, this study allows us to better understand the fundamental features of the EW process of the 12Cr18Ni10Ti – Titanium – AlMg6 multilayer composite material.

5. Funding

This work was supported by Russian Science Foundation No. 23-19-00446, https://rscf.ru/project/23-19-00446/

6. Conflict of interest

The authors declare no conflict of interest.

References

1. Wahid MA, Siddiquee AN, Khan ZA. Aluminum alloys in marine construction: characteristics, application, and problems from a fabrication viewpoint. *Marine Systems & Ocean Technology*. 2020;15(1):70-80. DOI:10.1007/s40868-019-00069-w
2. Matteis P, Gullino A, D'Aiuto F, Puro CM, et al. Welding between aluminum alloy and steel sheets by using transition joints. *Journal of Materials Engineering and Performance*. 2020;29(8):4840-4853. DOI:10.1007/s11665-020-04595-2
3. Groche P, Wohletz S, Brenneis M, Pabst C, et al. Joining by forming – a review on joint mechanisms, applications and future trends. *Journal of Materials Processing Technology*. 2014;214(10):1972-1994. DOI:10.1016/j.jmatprotec.2013.12.022
4. Gullino A, Matteis P, D'Aiuto F. Review of aluminum-to-steel welding technologies for car-body applications. *Metals*. 2019;9(3):315. DOI:10.3390/met9030315
5. Wu X, Shi C, Feng K, Gao L, et al. Experimental and numerical approach to titanium-aluminum explosive welding. *Materials Research Express*. 2021;8(9):096503. DOI:10.1088/2053-1591/ac2017
6. Wang K, Kuroda M, Chen X, Hokamoto K, et al. Mechanical properties of explosion-welded titanium/duplex stainless steel under different energetic conditions. *Metals*. 2022;12(8):1354. DOI:10.3390/met12081354
7. Carvalho GHSFL, Galvão I, Mendes R, Leal RM, et al. Aluminum-to-steel cladding by explosive welding. *Metals*. 2020;10(8):1062. DOI:10.3390/met10081062
8. Amani H, Soltanieh M. Intermetallic phase formation in explosively welded Al/Cu bimetals. *Metallurgical and Materials Transactions B*. 2016;47(4):2524-2534. DOI:10.1007/s11663-016-0682-1
9. Chen X, Inao D, Tanaka S, Mori A, et al. Explosive welding of Al alloys and high strength duplex stainless steel by controlling energetic conditions. *Journal of Manufacturing Processes*. 2020;58:1318-1333. DOI:10.1016/j.jmapro.2020.09.037
10. Aizawa Y, Nishiwaki J, Harada Y, Muraishi S, et al. Experimental and numerical analysis of the formation behavior of intermediate layers at explosive welded Al/Fe joint interfaces. *Journal of Manufacturing Processes*. 2016;24:100-106. DOI:10.1016/j.jmapro.2016.08.002
11. Aceves SM, Espinosa-Loza F, Elmer JW, Huber R. Comparison of Cu, Ti and Ta interlayer explosively fabricated aluminum to stainless steel transition joints for cryogenic pressurized hydrogen storage. *International Journal of Hydrogen Energy*. 2015;40(3):1490-1503. DOI:10.1016/j.ijhydene.2014.11.038
12. Malakhov A, Niyozbekov N, Denisov I, Saikov I, et al. Study of structure formation in multilayer composite material AA1070-AlMg6-AA1070-Titanium (VT1-0)-08Cr18Ni10Ti steel after explosive welding and heat treatment. *Journal of Manufacturing and Materials Processing*. 2024;8(5):188. DOI:10.3390/jmmp8050188
13. Malakhov A, Denisov I, Niyozbekov N, Saikov I, et al. Theoretical and experimental studies of the shock-compressed gas parameters in the welding gap. *Materials*. 2024;17(1):265. DOI:10.3390/ma17010265
14. Chu Q, Xia T, Zhao P, Zhang M, et al. Interfacial investigation of explosion-welded Al/steel plate: the microstructure, mechanical properties and residual stresses. *Materials Science and Engineering: A*. 2022;833:142525. DOI:10.1016/j.msea.2021.142525
15. Gao M, Chen T. Formation of intermetallic compounds during reaction between Ti and Al–Mg alloys with various Mg contents. *Journal of Materials Science & Technology*. 2023;159:225-243. DOI:10.1016/j.jmst.2023.02.052
16. O'Kelly P, Watson A, Schmidt G, Galetz M, et al. Ti-Fe phase evolution and equilibria toward β-Ti superalloys. *Journal of Phase Equilibria and Diffusion*. 2023;44(6):738-750. DOI:10.1007/s11669-023-01066-8
17. Massicot B, Joubert JM, Latroche M. Phase equilibria in the Fe–Ti–V system. *International Journal of Materials Research*. 2010;101(11):1414-1423. DOI:10.3139/146.110379
18. Zha Y, Zhang C, Zhu W, He X, et al. Experimental and numerical investigations on the microstructural features and mechanical properties of explosively welded aluminum/titanium/steel trimetallic plate. *Materials Characterization*. 2024;209:113669. DOI:10.1016/j.matchar.2024.113669
19. Chu Q, Cao Q, Zhang M, Zheng J, et al. Microstructure and mechanical properties investigation of explosively welded titanium/copper/steel trimetallic plate. *Materials Characterization*. 2022;192:112250. DOI:10.1016/j.matchar.2022.112250
20. Gloc M, Wachowski M, Plocinski T, Kurzydlowski KJ. Microstructural and microanalysis investigations of bond titanium grade1/low alloy steel st52-3N obtained by explosive welding. *Journal of Alloys and Compounds*. 2016;671:446-451. DOI:10.1016/j.jallcom.2016.02.120
21. Carvalho GHSFL, Galvão I, Mendes R, Leal RM, et al. Microstructure and mechanical behaviour of aluminium-carbon steel and aluminium-stainless steel clads produced with an aluminium interlayer. *Materials Characterization*. 2019;155:109819. DOI:10.1016/j.matchar.2019.109819
22. Bataev IA, Tanaka S, Zhou Q, Lazurenko DV, et al. Towards better understanding of explosive welding by combination of numerical simulation and experimental study. *Materials & Design*. 2019;169:107649. DOI:10.1016/j.matdes.2019.107649
23. Zhou Q, Liu R, Zhou Q, Ran C, et al. Effect of microstructure on mechanical properties of titanium-steel explosive welding interface. *Materials Science and Engineering: A*. 2022;830:142260. DOI:10.1016/j.msea.2021.142260

Information about the authors / Информация об авторах

Andrey Yu. Malakhov, Cand. Sc. (Eng.), Senior Researcher, Merzhanov Institute of Structural Macrokinetics and Materials Science, Russian Academy of Science (ISMAN), Chernogolovka, Russian Federation; ORCID 0000-0002-0567-7307; e-mail: sir.malahov2009@yandex.ru

Stepan A. Seropyan, Junior Research, ISMAN, Chernogolovka, Russian Federation; ORCID 0000-0002-3714-3983; e-mail: stepan.seropyan@yandex.ru

Igor V. Denisov, Cand. Sc. (Eng.), Senior Researcher, ISMAN, Chernogolovka, Russian Federation; ORCID 0000-0002-1065-3318; e-mail: denisov@ism.ac.ru

Denis V. Shakhray, Cand. Sc. (Phys. and Math.), Senior Researcher, Head of the Department of Extreme States of Matter, Federal Research Center of Problems of Chemical Physics and Medicinal Chemistry of Russian Academy of Sciences, Chernogolovka, Russian Federation; ORCID 0009-0006-1192-1157; e-mail: shakhray@icp.ac.ru

Olga D. Boyarchenko, Cand. Sc. (Phys. and Math.), Research Fellow, ISMAN, Chernogolovka, Russian Federation; ORCID 0000-0002-7543-7608; e-mail: boyarchenko@ism.ac.ru

Nemat N. Niyozbekov, Junior Research, ISMAN, Chernogolovka, Russian Federation; ORCID 0000-0003-1812-2930; e-mail: nemat199595@mail.ru

Evgenii I. Volchenko, Junior Research, ISMAN, Chernogolovka, Russian Federation; ORCID 0009-0002-0721-643X; e-mail: spec15@mail.ru

Малахов Андрей Юрьевич, кандидат технических наук, старший научный сотрудник, Институт структурной макрокинетики и проблем материаловедения им. А. Г. Мержанова РАН (ИСМАН), Черноголовка, Российская Федерация; ORCID 0000-0002-0567-7307; e-mail: sir.malahov2009@yandex.ru

Серопян Степан Арутюнович, младший научный сотрудник, ИСМАН, Черноголовка, Российская Федерация; ORCID 0000-0002-3714-3983; e-mail: stepan.seropyan@yandex.ru

Денисов Игорь Владимирович, кандидат технических наук, старший научный сотрудник, ИСМАН, Черноголовка, Российская Федерация; ORCID 0000-0002-1065-3318; e-mail: denisov@ism.ac.ru

Шахрай Денис Владимирович, кандидат физико-математических наук, старший научный сотрудник, заведующий отделом экстремальных состояний вещества, Федеральный исследовательский центр проблем химической физики и медицинской химии РАН, Черноголовка, Российская Федерация; ORCID 0009-0006-1192-1157; e-mail: shakhray@icp.ac.ru

Боярченко Ольга Дмитриевна, кандидат физико-математических наук, научный сотрудник, ИСМАН, Черноголовка, Российская Федерация; ORCID 0000-0002-7543-7608; e-mail: boyarchenko@ism.ac.ru

Ниёзбеков Неъмат Ниёзбекович, младший научный сотрудник, ИСМАН, Черноголовка, Российская Федерация; ORCID 0000-0003-1812-2930; e-mail: nemat199595@mail.ru

Волченко Евгений Игоревич, младший научный сотрудник, ИСМАН, Черноголовка, Российская Федерация; ORCID 0009-0002-0721-643X; e-mail: spec15@mail.ru

Received 11 February 2025; Revised 28 March 2025; Accepted 31 March 2025